Adenosine mediates IL-13–induced inflammation and remodeling in the lung and interacts in an IL-13–adenosine amplification pathway

See the related Commentary beginning on page 329.

Michael R. Blackburn,[1] Chun G. Lee,[2] Hays W.J. Young,[1] Zhou Zhu,[2] Janci L. Chunn,[1] Min Jong Kang,[2] Suman K. Banerjee,[1] and Jack A. Elias[2]

[1]Department of Biochemistry and Molecular Biology, University of Texas-Houston Medical School, Houston, Texas, USA
[2]Section of Pulmonary and Critical Care Medicine, Department of Internal Medicine, Yale University School of Medicine, New Haven, Connecticut, USA

IL-13 is an important mediator of inflammation and remodeling. We hypothesized that adenosine accumulation, alterations in adenosine receptors, and adenosine–IL-13 autoinduction are critical events in IL-13–induced pathologies. To test this, we characterized the effects of IL-13 overexpression on the levels of adenosine, adenosine deaminase (ADA) activity, and adenosine receptors in the murine lung. We also determined whether adenosine induced IL-13 in lungs from ADA-null mice. IL-13 induced an inflammatory and remodeling response that caused respiratory failure and death. During this response, IL-13 caused a progressive increase in adenosine accumulation, inhibited ADA activity and mRNA accumulation, and augmented the expression of the A_1, A_{2B}, and A_3 but not the A_{2A} adenosine receptors. ADA enzyme therapy diminished the IL-13–induced increase in adenosine, inhibited IL-13–induced inflammation, chemokine elaboration, fibrosis, and alveolar destruction, and prolonged the survival of IL-13–transgenic animals. In addition, IL-13 was strongly induced by adenosine in ADA-null mice. These findings demonstrate that adenosine and adenosine signaling contribute to and influence the severity of IL-13–induced tissue responses. They also demonstrate that IL-13 and adenosine stimulate one another in an amplification pathway that may contribute to the nature, severity, progression, and/or chronicity of IL-13 and/or Th2-mediated disorders.

J. Clin. Invest. **112**:332–344 (2003). doi:10.1172/JCI200316815.

Introduction

Inflammatory and remodeling responses are prominent features of disorders of the airway and parenchyma of the lung. These responses are readily apparent in asthma, which is characterized by an eosinophil and mononuclear cell–rich inflammatory response and airway remodeling (1, 2), and the interstitial lung diseases such as idiopathic pulmonary fibrosis (IPF), in which Th2-type inflammation and pulmonary fibrosis are juxtaposed (3, 4). They are also readily apparent in chronic obstructive pulmonary disease (COPD), which is characterized by inflammation with increased numbers of $CD8^+$ lymphocytes, macrophages, eosinophils, and granulocytes and a remodeling response with alveolar septal destruction, septal fibrosis, and changes in pulmonary compliance (5–8). In contrast to most injury and repair responses, the inflammation seen in these disorders is chronic and may last throughout the life of the afflicted individual. Surprisingly, the mechanisms that are responsible for the generation of each of these abnormalities have not been adequately defined, and the mechanisms that are responsible for their intensity and chronicity have not been elucidated.

Adenosine is a nucleoside that is generated by ATP catabolism at sites of tissue stress and injury including inflammation and tissue remodeling. Adenosine signals via G protein–coupled receptors that regulate a wide array of physiologic systems (9–11) and immune homeostasis (12–15). Elevated levels of adenosine are found in the bronchoalveolar lavage (BAL) fluid from patients with asthma (16), and adenosine regulates the function of a number of cell types central to this disorder, including mast cells (17), eosinophils (18), macrophages (19), neurons

Received for publication September 3, 2002, and accepted in revised form May 6, 2003.

Address correspondence to: Jack A. Elias, Section of Pulmonary and Critical Care Medicine, Department of Internal Medicine, Yale University School of Medicine, 300 Cedar Street, S441-C, New Haven, Connecticut 06520-8057, USA.
Phone: (203) 785-4163; Fax: (203) 785-3826;
E-mail: jack.elias@yale.edu.
M.R. Blackburn and C.G. Lee contributed equally to this work.

Conflict of interest: The authors have declared that no conflict of interest exists.

Nonstandard abbreviations used: idiopathic pulmonary fibrosis (IPF); chronic obstructive pulmonary disease (COPD); bronchoalveolar lavage (BAL); adenosine deaminase (ADA); transgenic (Tg); rat Clara cell 10-kDa protein (CC10); polyethylene glycol-modified ADA (PEG-ADA); monocyte chemotactic protein-3 (MCP-3); histologic mucus index (HMI); periodic acid-Schiff (PAS); thymus- and activation-regulated chemokine (TARC); stomal cell–derived factor-1 (SDF-1); mucin-5AC (MUC-5AC).

(20), epithelial cells (21), and smooth muscle cells (22). Aerosol adenosine exposure induces bronchospasm in patients with asthma and COPD, but not in normal controls (23, 24). In addition, recent studies from our laboratories demonstrated that mice with a null mutation of adenosine deaminase (ADA) (the enzyme that degrades adenosine) have elevated levels of tissue adenosine that generates a phenotype that is similar in important ways to the responses in asthma, COPD, and the interstitial disorders. This includes eosinophil- and macrophage-rich inflammation, alveolar enlargement, airway remodeling, mucus metaplasia, airway hyperresponsiveness after agonist challenge, and tissue fibrosis (25, 26). When viewed in combination, these studies strongly suggest that adenosine plays an important role in the pathogenesis of these disorders. The relationships between adenosine accumulation and the tissue inflammation and cytokine dysregulation that are characteristic of these disorders have not been defined, however. In addition, the role, if any, of adenosine in regulating the nature, severity, or chronicity of these responses has not been assessed.

IL-13 is a pleiotropic 12-kDa product of a gene on chromosome 5 at q31 that is produced in large quantities by Th2 cells. A large number of studies has demonstrated that IL-13 is overproduced in asthma and has implicated IL-13 in the pathogenesis of the Th2 inflammation and airway remodeling that is characteristic of this disorder (27–31). In addition, it had long been speculated that asthma and COPD are not distinct entities and that similar mechanisms may contribute to the pathogenesis of both diseases (27). The asthma- and COPD-relevant effector functions of IL-13 can be appreciated in studies from our laboratories that demonstrated that the lung-specific constitutive and/or inducible overexpression of IL-13 produced eosinophil-, lymphocyte-, and macrophage-rich inflammation, alveolar enlargement, mucus metaplasia, and airway hyperresponsiveness on methacholine challenge (28, 29). In keeping with studies highlighting the dysregulation of IL-13 in fibrotic lung disorders, transgenic IL-13 is also a potent inducer of tissue fibrosis (4, 29–32). The mechanisms that are responsible for IL-13–induced inflammatory, proteolytic, and fibrotic responses, however, are not adequately understood. In addition, despite the strikingly similar phenotypes engendered by the overexpression of IL-13 and a null mutation of ADA (25, 26, 28, 29), the importance of adenosine in the generation of IL-13–induced tissue inflammation has not been investigated, and the role of IL-13 in the pathogenesis of adenosine-induced tissue responses has not been characterized. Lastly, the ways that IL-13 and adenosine interact to regulate the character, intensity, and chronicity of inflammatory and remodeling disorders of the lung have not been described.

We hypothesized that adenosine plays an important role in the pathogenesis of IL-13–induced tissue alterations and that IL-13 and adenosine can regulate one another in respiratory tissues. To test this hypothesis we (a) characterized the metabolism of adenosine in lungs from transgenic (Tg) mice in which IL-13 was overexpressed in a lung-specific fashion, (b) defined the contributions of adenosine in the genesis of the IL-13–induced alterations in these animals, and (c) characterized the expression of IL-13 in lungs from ADA-deficient and control animals. These studies demonstrate that adenosine accumulation, downregulation of ADA, and adenosine receptor alterations play important roles in the pathogenesis of IL-13–induced phenotypes in the lung. They also demonstrate that adenosine is a potent stimulator of IL-13, which highlights a pathway via which IL-13 and adenosine can stimulate one another.

Methods

Transgenic mice. Studies were conducted using the rat Clara cell 10-kDa protein–IL-13 (CC10-IL-13) Tg mice that were generated on a C57BL/6 background. These mice use the CC10 promoter to overexpress murine IL-13 in a lung-specific fashion (29). In these mice IL-13 causes progressive pulmonary pathology characterized by eosinophilic and mononuclear inflammation, alveolar enlargement, mucus metaplasia, and airway fibrosis (29, 33). As a consequence of this response these mice die prematurely from respiratory failure at approximately 3.5–4 months of age (33). Non-Tg littermates were used as controls. Genotyping was conducted by screening genomic DNA isolated from tail biopsies using PCR as described previously (33).

Adenosine quantification. Mice were anesthetized, a median sternotomy was undertaken, and the lungs were rapidly removed and frozen in liquid nitrogen. Adenine nucleosides were extracted from frozen lung tissue using 0.4 N perchloric acid as described previously (34). Adenosine was separated and quantified using reversed-phase HPLC (35).

ADA enzyme therapy and analysis of ADA enzyme activity. Polyethylene glycol–modified ADA (PEG-ADA), also known as Adagen, was obtained through collaboration with Enzon Inc. (Piscataway, New Jersey, USA). Mice were randomized to receive intraperitoneal or intranasal injections of PEG-ADA or a vehicle control. The route of delivery was chosen based on the end points that were being examined. The intraperitoneal dosing regimen consisted of 15 U of PEG-ADA delivered every 4 days during the treatment period. The intranasal dose consisted of 5 U delivered every 4 days. These doses are within the range of dosages previously employed by our laboratories in ADA-deficient animals (36). In experiments in which inflammation was being assessed, intraperitoneal injections were started when the animals were 2 months of age, and the animals were sacrificed when they were 3 months old. For the survival studies, intraperitoneal injections were started in 2-month-old animals and continued until the animals died or were

5 months old. When alveolar remodeling and tissue fibrosis were being evaluated, intranasal instillations of enzyme or vehicle control were started in 2-month-old animals and maintained for 10 and 30 days, respectively. The levels of ADA enzyme activity in serum and tissues were measured using zymogram analysis and a spectrophometric enzymatic assay following established procedures (37). The effects of these interventions on the levels of tissue and BAL IL-13 were assessed using an ELISA kit per the manufacturer's directions (R&D Systems Inc., Minneapolis, Minnesota, USA).

BAL. Mice were euthanized, the trachea was isolated by blunt dissection, and a small-caliber tube was inserted into the airway and secured. Two volumes of 1 ml of PBS with 0.1% BSA were instilled and gently aspirated and pooled (BAL fluid). Samples were then centrifuged at 1,250 *g* for 5 minutes to recover cells, and the supernatants were collected and stored at –70°C for further analysis. Cell pellets were resuspended in PBS and total cell counts determined using a hemocytometer. Aliquots were cytospun onto microscope slides and stained for cellular differentials.

Analysis of mRNA. Mice were anesthetized, and the lungs were rapidly removed and frozen on liquid nitrogen. RNA was isolated from frozen lungs using TRIzol Reagent (Life Technologies Inc., Grand Island, New York, USA) according to the manufacturer's instructions. RNA samples were then DNase treated and subjected to either semiquantitative or quantitative real-time RT-PCR. The primers used for semiquantitative RT-PCR for ADA and adenosine receptors were as follows: ADA sense, 5′-GGCGTGGTCTATGTGGAAGT-3′, antisense, 5′-TGATAACCATGTCCCACCCT-3′; A1 receptor sense, 5′-GCAGGCACTGCATCACTTTA-3′, antisense, 5′-ACCTTCACAGCCCAAATCAC-3′; A_{2A} receptor sense, 5′-CACGCAGAGTTCCATCTTCA-3′, antisense, 5′-GTTGGCTCTCCATCTGCTTC-3′; A_{2B} receptor sense, 5′-CATTACAGACCCCCACCAAC-3′, antisense, 5′-GGACAGCAGCTTTTATTCGC-3′; and A_3 receptor sense, 5′-ATATGGCTATTCCTGGGCCT-3′, antisense, 5′-GGCACAAAAGAGTGCTGCTA-3′. The primers, probes and procedures for real-time RT-PCR for the adenosine receptors and monocyte chemotactic protein-3 (MCP-3) and the RT-PCR for chemokines were described previously (26, 33).

Histology. Tissues were fixed overnight in 10% buffered formalin. After washing in fresh PBS, fixed tissues were dehydrated, cleared, and embedded in paraffin by routine methods. Sections (5 μm) were collected on Superfrost Plus positively charged microscope slides (Fisher Scientific Co., Houston, Texas, USA), deparaffinized, and stained with H&E or Mallory's trichrome as described previously (38, 39).

MCP-3 immunohistochemistry. Paraffin-embedded lungs were sectioned (5 μm) and collected on Superfrost Plus positively charged microscope slides. Deparaffinized, sections were rehydrated in a series of graded alcohols ending in water. Antigen unmasking was performed using a target-retrieval solution following the manufacturer's guidelines (DAKO Corp., Carpinteria, California, USA), and endogenous peroxidase activity was blocked by incubation in 0.3% H_2O_2 in PBS for 30 minutes. Localization was undertaken by incubating tissue sections for 30 minutes at room temperature with a 1:4 dilution of goat anti-mouse MARC (MCP-3) Ab (R&D Systems Inc.) (40) followed by development with a goat IgG Vectastain Elite ABC Kit (Vector Laboratories, Burlingame, California, USA) as described by the manufacturer.

In situ hybridization. Paraffin-embedded lungs were sectioned (5 μm) and collected on Superfrost Plus positively charged microscope slides. After they were deparaffinized, in situ hybridization was carried out according to established protocols (41). The cDNA clones used to generate riboprobes for the murine A_1 and A_{2B} adenosine receptors were provided by Diana Marquardt (University of California at San Diego, San Diego, California, USA). A portion of the A_3 adenosine receptor cDNA was obtained from Marlene Jacobson (Merck Pharmaceuticals, West Point, Pennsylvania, USA). Plasmids were linearized and either T3 or T7 RNA polymerase was used to generate antisense and sense riboprobes labeled with [α-^{35}S]UTP. Samples were overlaid with 8 million counts of antisense or sense riboprobe and hybridized overnight at 60°C. Posthybridization washes were carried out as described (41), and slides were dipped in Kodak NTB-2 emulsion and exposed for 1–4 weeks. Sections were viewed and photographed using an Olympus BX60 microscope equipped with a SPOT digital camera (Diagnostics Instruments, Sterling Heights, Michigan, USA).

Assessment of lung volume and alveolar size. To evaluate the effects of IL-13 and adenosine on parameters of alveolar remodeling, lung volume and alveolar size were evaluated as described previously by our laboratory (28). For the volume measurements, the animals were anesthetized, the tracheas were cannulated, and the lungs were degassed. The lungs and heart were then removed en bloc and inflated with PBS at 30 cm of pressure. The size of the lung was evaluated via volume displacement.

Alveolar size was estimated from the mean cord length of the air space. In these evaluations, sections were prepared as described above, images were acquired into a Macintosh computer through a framegrabber board in 8-bit grayscale at a final magnification of 1.5 pixels per micrometer and analyzed using the public domain NIH Image program written by Wayne Rasband at the NIH (available at http://rsb.info.nih.gov/nih-image using a custom-written macro available from the website). Images had a threshold set manually and were then smoothed and inverted. The image was then subject to sequential logical image match "AND" operations with a horizontal and then vertical grid. At least 200 measurements per field were made in transgene-positive animals, and 400 measurements per field were made in the transgene-negative animals. The length

of the lines overlying air space was averaged as the mean chord length.

Quantification of lung collagen. Lung collagen content was determined by quantifying total soluble collagen using the Sircol Collagen Assay kit (Biocolor Ltd., Belfast, Northern Ireland) as described previously by our laboratory (38, 39). In accordance with the manufacturer's instructions, lungs were homogenized in 5 ml of 0.5 M acetic acid containing 1 mg pepsin (Sigma-Aldrich, St. Louis, Missouri, USA) per 10 mg tissue residue. Each sample was incubated for 24 hours at 4°C with stirring. After centrifugation, 100 μl of each supernatant was assayed. One milliliter of Sircol dye reagent, which specifically binds to collagen, was then added to each sample and mixed for 30 minutes. After centrifugation, the pellet was suspended in 1 ml of alkali reagent (0.5 M NaOH) included in the kit, and optical density was evaluated at 540 nm with a spectrophotometer. The values in the test samples were compared with the values obtained with collagen standard solutions provided by the manufacturer, which were used to construct a standard curve.

Quantification of mucus metaplasia and BAL mucins. Mucus metaplasia was assessed by calculating the histologic mucus index (HMI), which provides a measurement of the percentage of epithelial cells that are positive for periodic acid–Schiff (PAS) with diastase per unit of airway basement membrane. It is calculated from PAS-stained sections as described previously by our laboratories (28, 39).

The mucin-5AC (MUC-5AC) in BAL fluids from transgene-positive and transgene-negative mice was quantitated as described previously by our laboratory (39). In brief, serial dilutions (0.1 ml) of BAL fluid was slot blotted onto nitrocellulose membranes using a Minifold II slot-blot apparatus (Schleicher & Schuell Inc., Keene, New Hampshire, USA). After air drying, the membrane was blocked with 5% skim milk for 2 hours, washed, and incubated overnight at 4°C with a mAb against MUC-5AC (45M1; Lab Vision Corp., Fremont, California, USA). After four additional washes, the membranes were incubated for 1 hour at room temperature with horseradish peroxidase–conjugated anti-mouse IgG (Pierce Chemical Co., Rockford, Illinois, USA). Immunoreactive mucins were detected using a chemiluminescent procedure (ECL Plus Western Blotting Detection System; Amersham Life Sciences Inc., Arlington Heights, Illinois, USA) and quantitated by densitometry.

Quantification of IL-13 in ADA-null mice and theophylline treatment. ADA-deficient mice on a mixed 129/SV and C57BL/6J background were generated and genotyped as described previously (34, 42). Littermates were used as controls. At 3 weeks of age lungs were harvested from wild-type and ADA-deficient mice, and whole-lung RNA was isolated as described above. A subset of 3-week-old ADA-deficient mice were treated with 10 U of PEG-ADA, and lung RNA was isolated 72 hours later. For theophylline treatments, mice were maintained on ADA enzyme therapy from birth, and at 3 weeks of age enzyme therapy was stopped and Alzet osmotic pumps containing saline or theophylline (625 ng/h/mouse release rate) were implanted. RNA was collected from lungs 12 days after the cessation of enzyme therapy. IL-13 mRNA was then quantitated using semiquantitative RT-PCR as previously described (39) or quantitative real-time RT-PCR. The RT-PCR primers that were used were sense, 5′-AGACCAGACTCCCCTGTGCA-3′, and antisense, 5′-TGGGTCCTGTAGATGGCATTG-3′. For quantitative real-time RT-PCR a Quantitech SYNBER Green RT-PCR kit (QIAGEN Inc., Valencia, California, USA) was used, and reactions were carried out on a Smart Cycler rapid thermal cycler system (Cepheid, Sunnyvale, California, USA). Data were analyzed using Smart Cycler analysis software using an internal standard curve, and final data were presented as mean nanograms of IL-13 mRNA per micrograms of total RNA.

Results

Adenosine levels in lungs from IL-13 Tg mice. To determine if IL-13 regulated pulmonary adenosine accumulation, adenosine levels were quantified in lungs from 1- to 3-month-old wild-type and *IL-13 Tg* mice. At 1 month of age, there was no difference in the adenosine levels in lungs from wild-type and *IL-13 Tg* mice. By 2 months of age, however, a significant increase in adenosine concentration was seen in lungs from *IL-13 Tg* animals (Figure 1). By 3 months of age, adenosine concentrations in lungs from *IL-13 Tg* mice had increased to levels tenfold greater than those measured in wild-type lungs. Adenosine levels were not elevated in the serum or the livers of *IL-13 Tg* mice at any time point (data not shown), illustrating that adenosine accumulation was limited to the lung where inflammation and damage were prominent. These findings demonstrate that adenosine concentrations

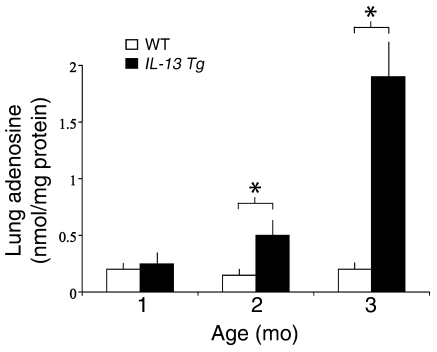

Figure 1
Lung adenosine levels are increased in *IL-13 Tg* mice. Adenosine levels were quantified in lungs from Tg CC10-IL-13 mice at 1, 2, and 3 months of age. Non-Tg (WT) littermates were used as controls. Mean values are given as nanomoles of adenosine per milligram of protein ± SE. $n = 4$ for 1- and 2-month time points; $n = 6$ for the 3-month time point. Statistical significance was determined using Student t test analysis; $^*P = 0.005$.

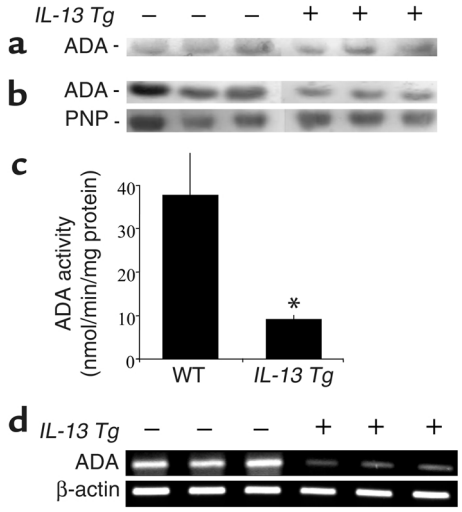

Figure 2
ADA expression is decreased in lungs from *IL-13 Tg* mice. (**a**) Serum was collected from 3-month-old wild-type, transgene-negative (–), or *IL-13 Tg*–positive (+) mice and subjected to zymogram analysis to examine levels of circulating ADA enzymatic activity. (**b**) ADA enzymatic activity was assessed in crude protein extracts from lungs from 3-month-old transgene-negative (–) and transgene-positive (+) mice using a zymographic assay system. Purine nucleoside phosphorylase (PNP) was used as a positive control for a purine metabolic enzyme that did not change. (**c**) ADA enzymatic activity was determined in lung extracts using a spectrophotometric assay. ADA-specific activities are shown and represent nanomoles of adenosine converted to inosine per minute per microgram of protein ± SE. $n = 4$ for each group. *$P = 0.05$ using Student t test. (**d**) Total cellular RNA was isolated from the lungs of 3-month-old transgene-negative (–) or transgene-positive (+) mice and subjected to RT-PCR using primers specific for ADA.

increase over time in lungs from *IL-13 Tg* mice. They also demonstrate that the levels of adenosine correlate with the intensity and severity of the IL-13–induced response in these animals.

ADA in lungs from IL-13 Tg mice. ADA is a major enzyme responsible for controlling the levels of adenosine in tissues and cells (43). To determine if the accumulation of adenosine in lungs from *IL-13 Tg* mice was associated with alterations in ADA, we quantified ADA enzymatic activity and the levels of mRNA encoding ADA in lungs from *IL-13 Tg* mice and littermate controls. ADA enzymatic activity was similar in the serum of wild-type and *IL-13 Tg* mice (Figure 2a). In contrast, there was a significant decrease in ADA parameters in lungs from 3-month-old *IL-13 Tg* animals. This decrease was readily apparent in assays for ADA enzymatic activity on lung extracts. Decreases were visualized using zymogram gel analysis (Figure 2b) and were verified using spectrophometric assays (Figure 2c). This decrease was at least partially specific for ADA since the activity of purine nucleoside phosphorylase, a downstream enzyme in purine catabolism, did not change (Figure 2b). Pretranslational mechanisms also appeared to be involved in this alteration because the levels of mRNA encoding ADA were decreased in lungs from 3-month-old *IL-13 Tg* mice (Figure 2d). These data demonstrate that ADA enzymatic activity and the levels of mRNA encoding ADA are decreased in the lungs from *IL-13 Tg* mice and suggest that these alterations contribute to the elevations in adenosine that are seen in these animals.

Expression of adenosine receptors in lungs from IL-13 Tg mice. Most of the effects of adenosine are mediated by cell surface adenosine receptors (44). To further understand the mechanism(s) by which adenosine could contribute to the pathogenesis of the tissue alterations induced by IL-13, we examined the expression of adenosine receptors in the lungs of these animals. At 3 months of age, transcripts for all four adenosine receptors were detected in RNA extracts from wild-type lungs (Figure 3a). Transcript levels for

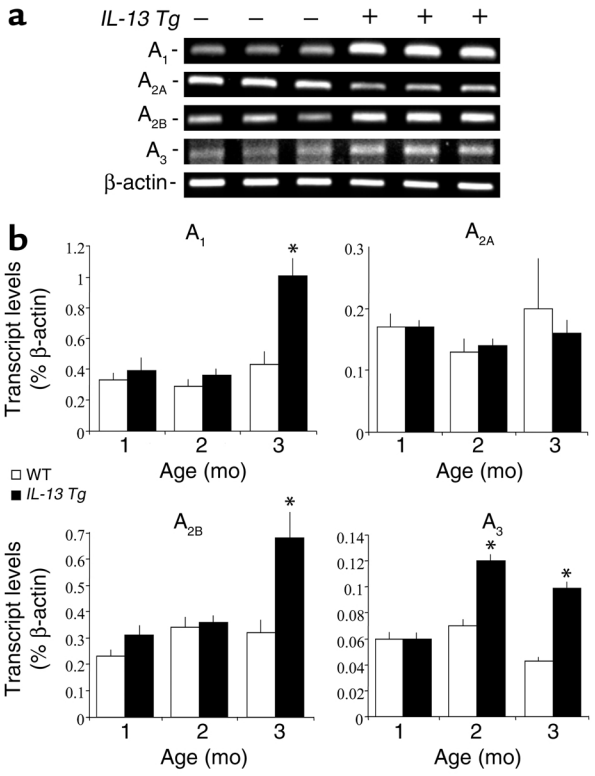

Figure 3
Alterations in adenosine receptor transcript levels in the lungs of *IL-13 Tg* mice. (**a**) Total cellular RNA was isolated from the lungs of 3-month-old wild-type (–) or *IL-13 Tg* mice (+) and subjected to RT-PCR using primer pairs specific for the four adenosine receptors. (**b**) Transcript levels for the A_1, A_{2A}, A_{2B}, and A_3 adenosine receptors were quantified using real-time RT-PCR in RNA isolated from whole lungs from wild-type and Tg mice at 1, 2, and 3 months of age. Values were normalized to β-actin transcript levels and are presented as the mean percentage of β-actin transcripts ± SE. Statistical significance was determined using Student t test analysis comparing wild-type to control values at each time point. $n = 4$ for each condition. *$P < 0.005$.

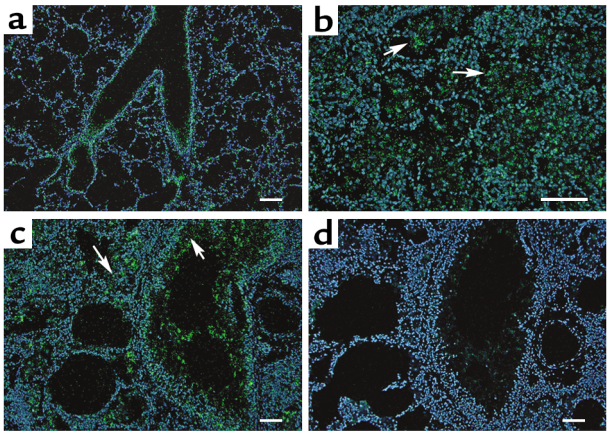

Figure 4
Expression of the A_1 adenosine receptor in the lungs of *IL-13 Tg* mice. (**a**) Dark-field image of a 3-month-old wild-type lung hybridized with an antisense cRNA probe specific for the A_1 adenosine receptor. (**b**) High magnification of a distal portion of a 3-month-old *IL-13 Tg* lung hybridized with antisense A_1 probe. Arrowheads denote inflammatory cells. (**c**) Three-month *IL-13 Tg* lung hybridized with antisense A_1 probe. Arrowheads denote airway epithelial cells. (**d**) Serial section of lung shown in **c** hybridized with a sense cRNA probe specific for the A_1 adenosine receptor. Green pixels denote specific hybridization, while blue epifluorescence represents nuclei stained with Hoechst 33258. Scale bars: 100 μm.

the A_{2A} adenosine receptor were decreased in the lungs of 3-month-old *IL-13 Tg* mice, whereas transcripts for the A_1, A_{2B}, and A_3 adenosine receptors were elevated (Figure 3a). To accurately quantify receptor transcript levels during the progression of lung inflammation and damage, real-time RT-PCR was also used. All four adenosine receptors were expressed at constant levels in wild-type lungs at 1, 2, and 3 months of age (Figure 3b). In contrast, the A_1 and A_{2B} adenosine receptors were markedly elevated in IL-13 lungs at 3 months of age, while the A_3 adenosine receptor was elevated at both 2 and 3 months of age (Figure 3b). These data demonstrate an increase in A_1, A_{2B}, and A_3 receptor expression in the lungs of *IL-13 Tg* mice, suggesting a heightened potential for adenosine signaling in these inflamed tissues.

In situ hybridization was next used to localize transcripts for the adenosine receptors in lungs from 3-month-old wild-type and *IL-13 Tg* mice. Expression of the A_1 adenosine receptor was localized to airway epithelium in wild-type mice (Figure 4a). This receptor was found in high concentrations in patches of inflammatory cells and in mucus containing airway epithelium of *IL-13 Tg* mice (Figure 4, b and c). The A_{2A} receptor was expressed diffusely throughout the lungs of both wild-type and *IL-13 Tg* mice (data not shown). Transcripts for the A_{2B} adenosine receptor were abundant in the bronchial epithelium of medium and large airways of wild-type lungs (Figure 5a). In the *IL-13 Tg* mice A_{2B} transcripts were found in inflammatory cells, likely macrophages, located within the enlarged alveolar spaces and in bronchial epithelium and walls of pulmonary blood vessels (Figures 5, b and c). The A_3 adenosine receptor was expressed diffusely in the lungs of wild-type mice (Figure 6a). In lungs from *IL-13 Tg* mice this receptor was expressed diffusely in the interstitium (data not shown) and in patches of inflammatory cells that encompassed eosinophils and macrophages near sites of remodeling (Figure 6b). Marked expression was also found in the epithelium of bronchial airways exhibiting mucus metaplasia (Figure 6c). These findings demonstrate that the elevations in adenosine receptor expression in lungs from *IL-13 Tg* mice are cell specific and noted on structural and inflammatory cells near sites of inflammation, remodeling, and mucus metaplasia.

Effects of ADA enzyme therapy on lung inflammation. Tg mice were treated with ADA enzyme replacement therapy to begin to assess the contributions of the elevated levels of adenosine to the pathogenesis of the IL-13–induced alterations in our modeling system. In these experiments, wild-type and *IL-13 Tg* mice were given intraperitoneal injections of PEG-ADA starting at 2 months of age, the time point at which adenosine levels began to increase in lungs from *IL-13 Tg* animals (Figure 1). After this 1-month intervention, adenosine concentrations in lungs from *IL-13 Tg* mice were reduced to values that were near, but still greater than, those in lungs from 3-month-old wild-type animals (Figure 7). Examination of the cellularity in BAL fluid

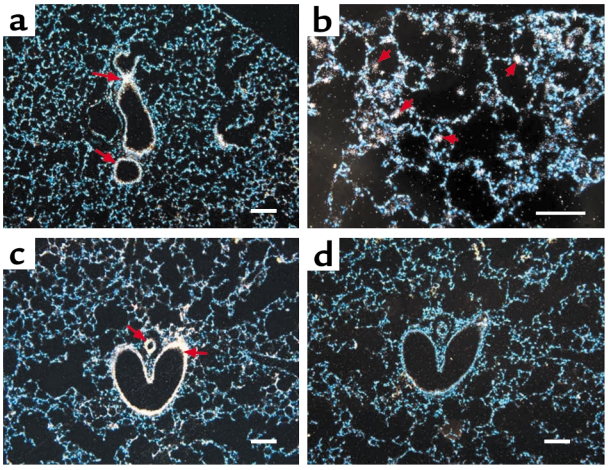

Figure 5
Expression of the A_{2B} adenosine receptor in the lungs of *IL-13 Tg* mice. (**a**) Dark-field image of a 3-month-old wild-type lung hybridized with an antisense cRNA probe specific for the A_{2B} adenosine receptor. Arrows denote expression in bronchial epithelium. (**b**) High-magnification of a distal portion of a 3-month-old *IL-13 Tg* lung hybridized with antisense A_{2B} probe denoting expression in alveolar macrophages (arrowheads). (**c**) Three-month *IL-13 Tg* lung hybridized with antisense A_{2B} probe. Arrows denote expression in bronchial epithelium and blood vessels. (**d**) Serial section of lung shown in **c** hybridized with a sense cRNA probe specific for the A_{2B} adenosine receptor. White pixels denote specific hybridization, while blue epifluorescence represents nuclei stained with Hoechst 33258. Scale bars: 100 μm.

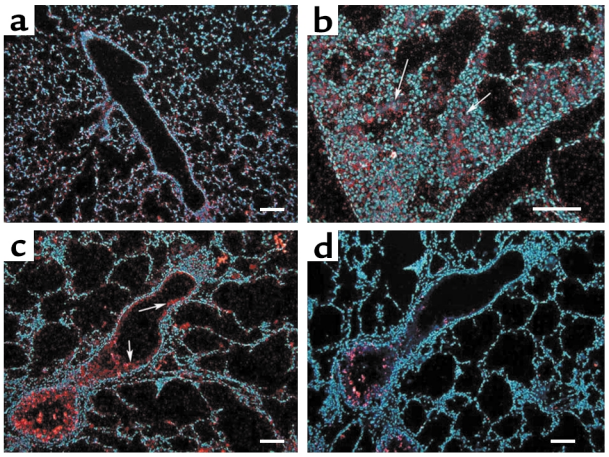

Figure 6
Expression of the A_3 adenosine receptor in the lungs of *IL-13 Tg* mice. (**a**) Dark-field image of a 3-month-old wild-type lung hybridized with an antisense cRNA probe specific for the A_3 adenosine receptor. (**b**) High magnification of a distal portion of a 3-month-old *IL-13 Tg* lung hybridized with antisense A_3 probe denoting expression in regions of inflammation and remodeling (arrows). (**c**) Three-month-old *IL-13 Tg* lung hybridized with antisense A_3 probe. Arrows denote expression in hypertrophied epithelium of the bronchial airways. (**d**) Serial section of lung shown in **c** hybridized with a sense cRNA probe specific for the A_3 adenosine receptor. Red pixels denote specific hybridization, while blue epifluorescence represents nuclei stained with Hoechst 33528. Scale bars: 100 μm.

revealed that ADA enzyme intervention was able to inhibit the accumulation of inflammatory cells in the lungs of *IL-13 Tg* mice (Figure 8a). After 1 month of treatment, the total number of cells recovered from the lungs from *IL-13 Tg* mice treated with PEG-ADA were less than 25% of the cells recovered from lungs from untreated *IL-13 Tg* mice. Differential counts revealed a reduction in macrophages, lymphocytes, and eosinophils recovered from the lungs of PEG-ADA–treated *IL-13 Tg* mice (Figure 8b). In agreement with our findings in BAL fluid, ADA enzyme therapy also substantially diminished the parenchymal inflammation in lungs from *IL-13 Tg* mice (Figure 8c). Importantly, these alterations were due to alterations in IL-13 effector pathway activation because ADA enzyme therapy did not alter the levels of BAL or lung lysate IL-13 (data not shown). These findings demonstrate that ADA enzyme therapy, while normalizing the levels of adenosine, inhibits the accumulation of inflammatory cells in lungs from *IL-13 Tg* mice.

Effects of ADA enzyme therapy on lung remodeling. To determine if the elevated levels of adenosine contributed to the pathogenesis of IL-13–induced alveolar remodeling and pulmonary fibrosis, we randomized Tg mice to 10 days and 30 days of therapy with intranasal PEG-ADA or vehicle control, respectively. As can be seen in Figure 9, a and b, IL-13 caused an impressive increase in lung volume and alveolar chord length. In both cases, PEG-ADA therapy markedly ameliorated these IL-13–induced responses. Similarly, IL-13 caused a marked increase in lung collagen content and impressive subepithelial airway fibrosis (Figure 9, c–f). These responses were also markedly diminished by PEG-ADA administration (Figure 9, c–f). In all cases, ADA enzyme therapy did not alter the levels of IL-13 in BAL fluids or lung lysates (data not shown). Interestingly, PEG-ADA therapy did not alter the ability of IL-13 to induce mucus metaplasia because the HMI values and levels of mRNA encoding MUC-5AC were similar in Tg mice treated with PEG-ADA or vehicle control (data not shown). PEG-ADA therapy did, however, cause a modest decrease in mucin secretion into BAL fluid as assessed by immunoblot analysis (Figure 10). When viewed in combination, these studies demonstrate that PEG-ADA therapy selectively diminishes IL-13–induced alveolar enlargement, pulmonary fibrosis, and mucin secretion without altering IL-13–induced mucus metaplasia.

Effects of ADA enzyme therapy on survival. As demonstrated previously, Tg IL-13 causes progressive inflammatory and fibrodestructive pulmonary alterations that cause respiratory failure and premature death (33). To determine if ADA enzyme therapy could extend the life span of IL-13 Tg mice, the survival of PEG-ADA and vehicle control–treated Tg mice were evaluated. In these experiments, Tg mice were randomized to intraperitoneal PEG-ADA or vehicle control at 2 months of age and maintained on this regimen for the rest of their lives. This regimen was chosen to stimulate the use of PEG-ADA therapy in patients with established disease. Despite our use of a protocol in which Tg IL-13 was produced in the murine lung for 2 months before therapy was initiated, PEG-ADA caused a significant increase in animal survival. Fifty percent of vehicle control-treated Tg mice were dead by 130 days of age, and 100% were dead by 150 days of age (Figure 11). In contrast, 50% of the ADA-treated mice lived for more than 165 days, and 25% were still alive at 180 days ($P < 0.03$). These data demonstrate that ADA enzyme therapy can significantly impact the severity of the lung disease in IL-13 Tg mice.

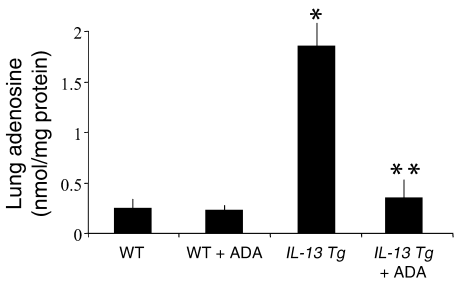

Figure 7
ADA enzyme therapy prevents adenosine accumulation in the lungs of *IL-13 Tg* mice. Two-month-old wild-type or *IL-13 Tg* mice were treated intraperitoneally with ADA enzyme therapy (+ ADA) for 1 month as described in Methods. At 3 months of age, adenosine levels were quantified in the lungs. Mean values are given as nanomoles of adenosine per milligram of protein ± SE. $n = 4$ for each group. *$P < 0.05$ vs. WT using Student t test; **$P < 0.01$ vs. *IL-13 Tg*.

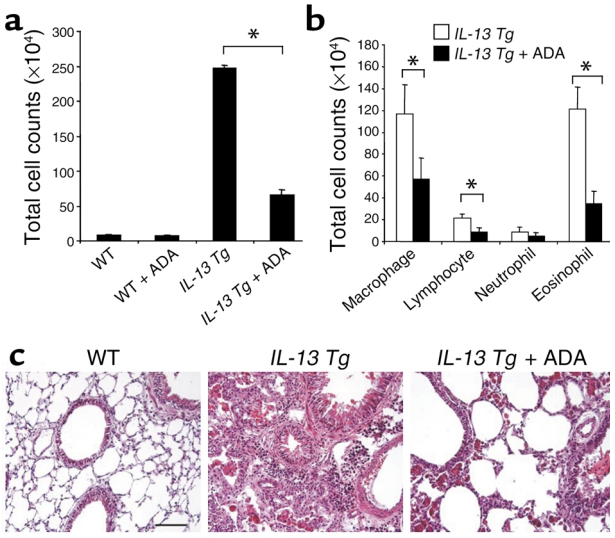

Figure 8
Effects of ADA enzyme therapy on the inflammation in lungs from *IL-13 Tg* mice. Two-month-old wild-type or *IL-13 Tg* mice were treated intraperitoneally with ADA enzyme therapy (+ ADA) for 1 month as described in Methods. At 3 months of age, the total numbers of cells (**a**) and the numbers of macrophages, lymphocytes, eosinophils, and neutrophils (**b**) recovered from the BAL fluid were determined. Values are given as mean total cell counts × 10^4 ± SE. Statistical significance was determined using Student *t* test analysis. $n = 6$ for each condition. *$P < 0.001$. (**c**) Representative H&E-stained sections through 3-month-old wild-type and *IL-13 Tg* lungs and 3-month-old *IL-13 Tg* lungs treated for 1 month with PEG-ADA. Similar results were seen in four different mice treated with PEG-ADA.

Chemokine expression in IL-13 Tg lungs. Previous studies from our laboratories demonstrated that IL-13 mediates its effects, in part, by its ability to stimulate the elaboration of a variety of chemokines and that chemokines such as MCP-3 are produced in an exaggerated fashion in association with elevated adenosine levels in the lungs from ADA-deficient mice (26, 33, 40). Thus, studies were undertaken to determine if adenosine played an important role in the ability of IL-13 to stimulate the production of MCP-3 and other IL-13–relevant chemokines. As shown in Figure 12, a and b, the levels of mRNA encoding MCP-1, MCP-2, MCP-3, MCP-5, eotaxin, eotaxin 2, thymus- and activation-regulated chemokine (TARC), and stromal cell–derived factor-1 (SDF-1) were augmented in comparisons of wild-type and Tg mice. Figure 12, b and c, also demonstrates that PEG-ADA treatment (1 month, intraperitoneal route) decreased the levels of mRNA encoding MCP-1, MCP-2, MCP-3, MCP-5, and eotaxin in lungs from IL-13 Tg mice. Similar results were seen with immunohistochemical evaluations that demonstrated that MCP-3 is readily appreciated in epithelial cells from *IL-13 Tg* mice and that the levels of MCP-3 protein decreased significantly after ADA therapy (Figure 12d). In contrast, PEG-ADA did not alter the levels of mRNA encoding TARC, eotaxin 2, or SDF-1 (Figure 12b). These findings demonstrate that IL-13 stimulates the production of selected chemokines including MCP-1, -2, -3, and -5 and eotaxin via an adenosine-dependent and ADA-regulatable activation pathway.

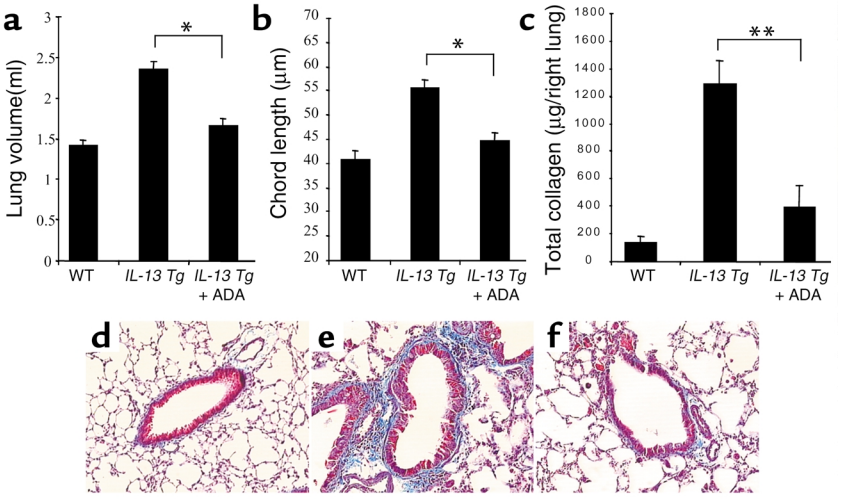

Figure 9
Effects of ADA enzyme therapy on the remodeling and fibrosis lungs from *IL-13 Tg* mice. Two-month-old wild-type or *IL-13 Tg* mice were treated with intranasal ADA enzyme therapy (+ ADA) for 10 days or with vehicle control. At the end of this interval, lung volume (**a**) and alveolar chord length (**b**) were evaluated as described in Methods. Values are given as mean ± SE. Statistical significance was determined using Student *t* test analysis. $n = 6$ for each condition. *$P < 0.001$. (**c**) Two-month-old wild-type or *IL-13 Tg* mice were treated with intranasal ADA enzyme therapy (+ ADA) for 30 days or with vehicle control. At the end of this interval, lung collagen content was assessed as described in Methods. Values are given as mean ± SE. Statistical significance was determined using Student *t* test analysis. $n = 6$ for each condition. *$P = 0.005$. (**d**–**f**) Two-month-old wild-type or *IL-13 Tg* mice were treated with intranasal ADA enzyme therapy for 30 days or with vehicle control. At the end of this interval, trichrome histologic evaluations of lung collagen were undertaken. The figure compares wild-type mice (**d**), Tg mice treated with vehicle (**e**), and Tg mice treated with PEG-ADA (**f**).

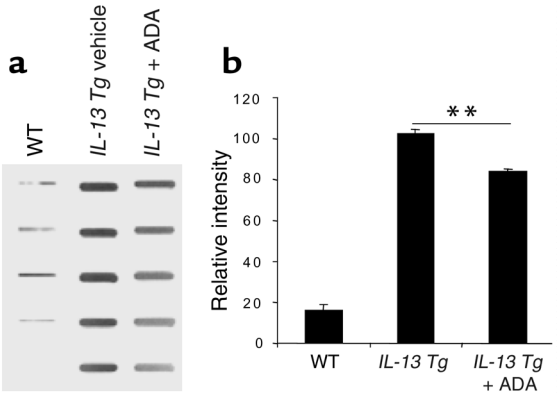

Figure 10
Effects of ADA enzyme therapy on BAL mucin secretion in lungs from *IL-13 Tg* mice Two-month-old wild-type or *IL-13 Tg* mice were treated with intranasal ADA enzyme therapy (+ ADA) or vehicle control for 10 days. At the end of this interval immunoblot analysis of BAL fluid was undertaken to quantify MUC-5AC as described in Methods. The immunoblot is on the left. Each row is representative of a different animal. The densitometric summary is on the right. $**P < 0.01$ using Student *t* test.

Adenosine receptor-dependent regulation of IL-13 levels in the lungs of ADA-deficient mice. The histopathologic features of lungs from ADA-deficient mice resemble those in lungs from IL-13 Tg mice (25, 26, 28, 29), suggesting that adenosine induction of IL-13 could be involved in phenotype generation in ADA-deficient animals. To begin to address this possibility, we compared the levels of mRNA encoding IL-13 in the lungs of ADA-deficient mice and littermate controls (Figure 13a). IL-13 transcripts were not detected in the lungs from wild-type littermate controls. In contrast, the levels of IL-13 mRNA were impressively elevated in the lungs of ADA-deficient mice, where they approximated the levels seen in lungs from 3-month-old *IL-13 Tg* animals. ADA-deficient mice were then treated with ADA enzyme therapy, which is known to lower lung adenosine concentrations and reverse many of the pulmonary pathologies seen in these mice (25). ADA enzyme therapy reversed the IL-13 mRNA accumulation in the lungs of ADA-deficient mice (Figure 13b), demonstrating that the IL-13 induction in this model is adenosine dependent. To evaluate the involvement of adenosine receptor signaling in this IL-13 inductive response, ADA-deficient mice were treated with the nonselective adenosine receptor antagonist, theophylline. This treatment prevented the accumulation of IL-13 in the lungs of these ADA-deficient animals (Figure 13c). These findings demonstrate that adenosine accumulation and subsequent signaling through adenosine receptors is a potent stimulator of IL-13 expression in the murine lung. They also suggest that adenosine-induced IL-13 may play an important role in the pathogenesis of the pulmonary alterations in ADA-deficient mice. When combined with our demonstration that IL-13 stimulates adenosine accumulation, these data highlight a positive feedback pathway in which IL-13 and adenosine can augment the accumulation of each other and, as a result, amplify and/or perpetuate local pathologic events.

Discussion

To further understand the cellular and molecular events that mediate the biologic effects of IL-13, we used a chronic overexpression Tg system to test the hypothesis that adenosine accumulation and adenosine receptor alterations are crucial events in the pathogenesis of IL-13–induced tissue pathologies. Our studies verified this hypothesis by demonstrating previously unappreciated relationships between IL-13 and the systems controlling adenosine homeostasis. Specifically, they demonstrate, we believe for the first time, that the progressive inflammation, alveolar remodeling, and lung fibrosis induced by Tg IL-13 are associated with progressive and proportionate increases in the levels of tissue adenosine and the enhanced expression of the A_1, A_{2B}, and A_3 adenosine receptors. They also demonstrate that ADA enzyme therapy, which decreases the levels of tissue adenosine, inhibited IL-13–induced inflammation, alveolar remodeling, pulmonary fibrosis, and mucus secretion and enhanced the survival of *IL-13 Tg* animals. Lastly, they demonstrate that elevated levels of adenosine stimulate IL-13 elaboration highlighting the ability of IL-13 and adenosine to mutually stimulate one another. These findings demonstrate that adenosine signaling can contribute to and influence the nature and severity of IL-13–induced lung pathologies. They also define an adenosine–IL-13 amplification pathway that may contribute to the severity, progression, consequences, and chronicity of IL-13– and Th2-mediated diseases and disorders.

Adenosine levels are controlled by the rates of adenosine production and adenosine catabolism. Extracellular adenosine is formed from the dephosphorylation of adenine nucleotides that are released from inflammatory cells and damaged airway epithelial and other structural cells. Adenosine is also generated intracellularly and released through constitutively expressed

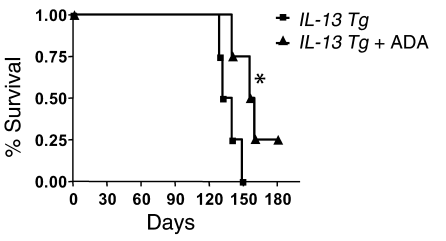

Figure 11
ADA enzyme therapy promotes the survival of *IL-13 Tg* mice. Two-month-old wild-type or *IL-13 Tg* mice were treated with ADA enzyme therapy (+ ADA), and survival was monitored as described in Methods. This is a representative experiment of $n = 4$. Statistical significance was determined using the Wilcoxon rank sum test. $n = 4$ for each group. $*P < 0.03$.

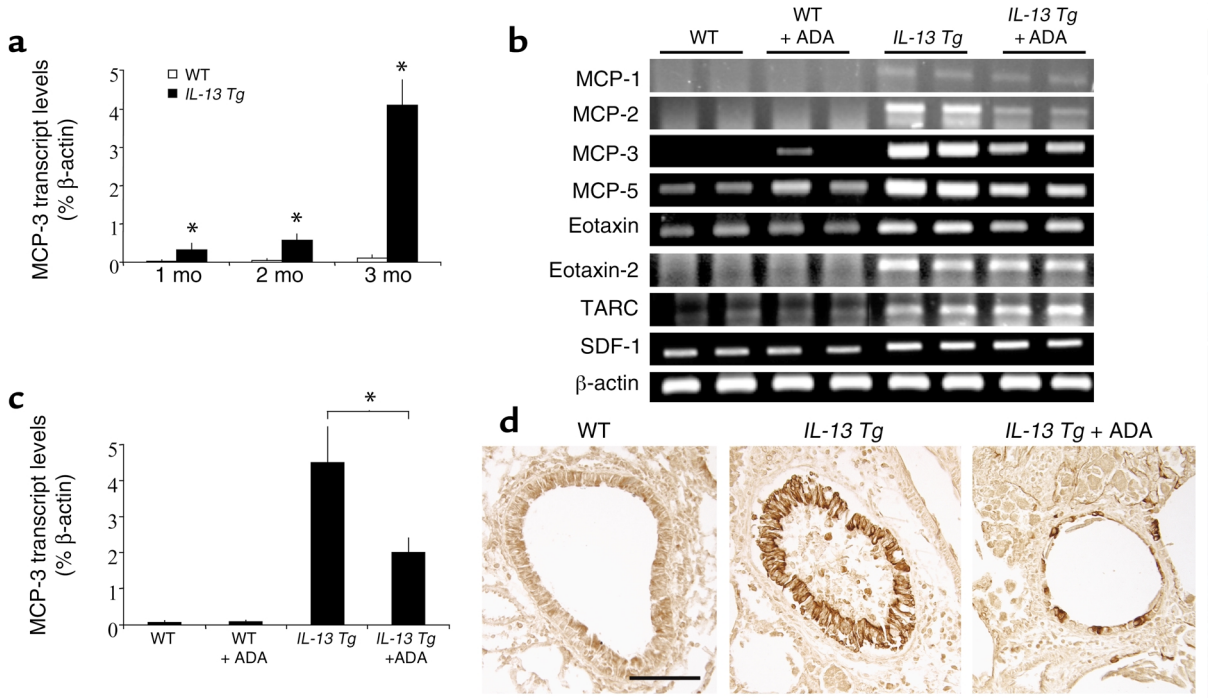

Figure 12
ADA enzyme therapy regulates chemokine expression in the lungs of *IL-13 Tg* mice. (**a**) MCP-3 transcript levels were quantified using real-time RT-PCR in RNA isolated from whole lungs from wild-type and Tg (*IL-13 Tg*) lungs at 1, 2, and 3 months of age. Values were normalized to β-actin transcript levels and are presented as the mean percentage of β-actin transcripts ± SE. Statistical significance was determined using Student *t* test analysis comparing wild-type to control values at each time point. $n = 4$ for each condition. $^*P = 0.005$. (**b**) RT-PCR analysis of the levels of mRNA encoding IL-13–relevant chemokines in whole-lung RNA from 3-month-old wild-type and *IL-13 Tg* mice treated with PEG-ADA (+ ADA) or vehicle for 1 month. (**c**) Quantitative real-time RT-PCR analysis of MCP-3 transcript levels in whole-lung RNA from 3-month-old wild-type and *IL-13 Tg* mice treated with PEG-ADA (+ ADA) or vehicle for 1 month. Values are presented as the mean percentage of β-actin transcripts ± SE. Statistical significance was determined using Student *t* test analysis. $^*P < 0.005$. $n = 4$ for each condition. (**d**) Immunohistochemistry was used to localize MCP-3 in lung sections from 3-month-old wild-type, *IL-13 Tg*, or *IL-13 Tg* mice treated with PEG-ADA for 1 month. Scale bar = 100 μm and applies to all three photographs in **d**.

nucleoside transporters. Once produced, adenosine can engage cell surface adenosine receptors or be removed by metabolism to inosine by cytosolic or extracellular ADA. Our studies demonstrate that adenosine levels increase significantly in lungs from *IL-13 Tg* mice (Figure 1). They also demonstrate that this increase in adenosine accumulation is associated with progressive tissue damage and fibrosis and impressive decreases in ADA activity and mRNA (Figure 2). These observations suggest that the heightened adenosine accumulation in lungs from IL-13 Tg mice is the result of a simultaneous increase in adenosine production and decrease in ADA-mediated adenosine catabolism. Interestingly, ADA enzymatic activity is elevated in the lungs of individuals with the prototypic Th1 inflammatory response caused by tuberculosis

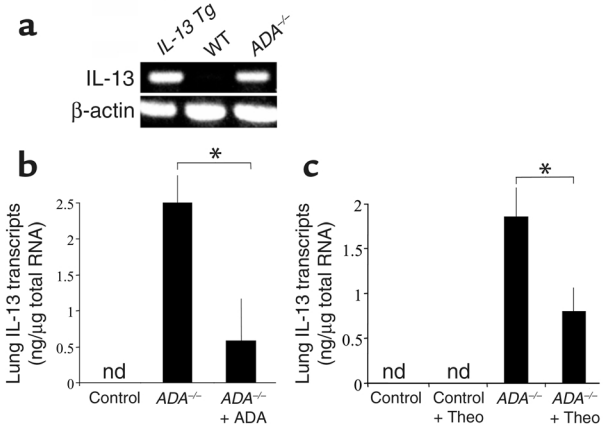

Figure 13
Adenosine-dependent elevations in IL-13 mRNA in lungs from ADA-deficient mice. (**a**) Whole-lung RNA was extracted from 3-month-old *IL-13 Tg* mice and 3-week old wild-type and ADA-deficient mice. RT-PCR was used to evaluate the levels of mRNA encoding IL-13 in these samples. (**b**) Three-week-old ADA-deficient ($ADA^{-/-}$) mice were treated with a single injection of PEG-ADA, and lung IL-13 mRNA levels were evaluated 72 hours later. IL-13 transcript values are presented as mean nanograms of IL-13 ± SE. $n = 5$ for each treatment. $^*P = 0.005$. (**c**) Control and ADA-deficient mice were maintained on ADA enzyme therapy for 3 weeks, and then Alzet pumps containing either theophylline (+ Theo) or saline were implanted. IL-13 mRNA levels were quantitated 12 days later. $n = 6$ for each treatment. $^*P = 0.05$. nd, not detected.

(45, 46). This suggests that differences in ADA levels and adenosine accumulation may represent a fundamental distinction between Th1- and Th2-driven inflammatory responses. Additional experimentation will be required to determine if ADA is differentially regulated in Th2 and Th1 responses and if ADA downregulation contributes to the elevated levels of adenosine in lungs from patients with asthma or COPD.

The regulatory effects of adenosine are mediated, to a great extent, by four G protein–coupled receptors that link ligand binding to a number of intracellular signaling pathways (44). The A_{2A} receptor is typically associated with anti-inflammatory effects of adenosine (47), while the A_1, A_{2B}, and A_3, adenosine receptors have been implicated in proinflammatory (48, 49) and bronchoconstrictive (22) adenosine responses. These findings demonstrate that the effects of adenosine are cell specific and depend on the type(s) of receptor that is activated. Our studies demonstrate that IL-13 causes striking changes in adenosine receptor expression in the murine lung, with the inhibitory A_{2A} receptor being unaltered or decreased, while the expression of the stimulatory A_1, A_{2B}, and A_3 receptors is markedly increased (Figures 3–6). They also demonstrate that the augmented receptor expression is not simply a function of the influx of inflammatory cells into the IL-13–treated lung because heightened adenosine receptor expression was noted on endothelial cells and epithelial cells as well as inflammatory cells such as macrophages and eosinophils (Figures 5 and 6). When viewed in combination, these receptor alterations would be expected to augment and or heighten adenosine-induced inflammation and airway remodeling. The A_3 adenosine receptor is expressed in an exaggerated fashion in tissues from patients with asthma and COPD (18). It is thus easy to see how the heightened expression of the A_1, A_{2B}, and A_3 receptors could have adverse effects in airway disorders such as asthma and COPD. It is also reasonable to speculate that receptor alterations such as these are responsible for and may be the basis of the well-documented bronchospastic response seen in patients with asthma and COPD but not in normal patients after aerosol adenosine challenge.

To define the contribution(s) of adenosine to the IL-13 phenotype we compared the inflammatory response and survival of IL-13 Tg mice that received and did not receive treatment with PEG-ADA. These studies demonstrated that inhibition of adenosine accumulation decreased lung inflammation and enhanced animal survival (Figures 8 and 11). These findings are similar to observations in ADA-deficient mice where PEG-ADA treatment was required to extend the life span and control the lung eosinophilia and macrophage accumulation in these animals (25). These studies demonstrate that adenosine is an important regulator of the intensity and severity of the chronic lung inflammation induced by IL-13. Recent studies from our laboratories demonstrated that IL-13 is a potent stimulator of MCP-3 and other chemokines and that signaling via their chemokine receptors plays a key role in the generation of IL-13 tissue responses (33). In the present studies we add to these observations and provide mechanistic insights by demonstrating that IL-13 induces MCP-1, MCP-2, MCP-3, MCP-5, MIP-1α, and eotaxin by an adenosine-dependent mechanism. These findings suggest that the ability of adenosine to regulate the production of selected chemokines is a key event in the generation of IL-13–induced inflammation. In accord with these observations, A_{2B} and A_3 receptor transcripts were abundant in airway epithelial cells from IL-13 Tg lungs (Figures 5 and 6); PKC and protein kinase A stimulate the production of MCP-3 (50); and A_{2B} and A_3 are known to activate both of these signaling pathways (44).

In addition to regulating tissue inflammation, IL-13 is being increasingly appreciated to be a major mediator of tissue remodeling (4, 28, 30). In accord with this appreciation, IL-13 is now felt to play an important role in the pathogenesis of the remodeling responses in asthma, COPD, schistosomiasis, nodular sclerosing Hodgkin disease, scleroderma, and idiopathic pulmonary fibrosis (28, 30–32, 51). To define the contributions of adenosine to these remodeling responses we compared the IL-13–induced remodeling in Tg animals that received and did not receive treatment with PEG-ADA. These studies demonstrate that IL-13–induced fibrosis and alveolar destruction were markedly decreased when adenosine levels were decreased with PEG-ADA. These findings have obvious therapeutic implications since they suggest that interventions that diminish adenosine may be useful therapeutically in fibrotic disorders such as IPF and diseases characterized by alveolar destruction such as COPD. Interestingly, these studies also demonstrate that the PEG-ADA interventions that were undertaken did not abrogate IL-13–induced mucus metaplasia and only moderately diminished IL-13–induced mucin secretion. On superficial analysis this would suggest that IL-13 induces mucus metaplasia via a pathway that is largely adenosine independent. This interpretation must be viewed with caution, however, because the ADA protocol that was used did not completely eliminate the IL-13–induced increase in tissue adenosine and was initiated in mice in which Tg IL-13 had been produced for 2 months prior to intervention. In addition, previous work from our laboratories has demonstrated that mucus metaplasia is the most sensitive feature of the in vivo IL-13 phenotype since it is seen with levels of BAL IL-13 as low as 20 pg/ml (52). Since our Tg mice had levels of BAL IL-13 between 300–500 pg/ml, our PEG-ADA intervention would need to be remarkably potent to diminish the functional capacity of the Tg IL-13 to below the 20 pg/ml threshold. When viewed in combination, these studies demonstrate that interventions that decrease lung adenosine diminish IL-13–induced lung fibrosis and tissue pro-

teolysis. Additional investigation will, however, be needed to define the contribution of adenosine to the pathogenesis of IL-13–induced mucus responses.

These studies were prompted by the appreciation that the phenotypes of *IL-13 Tg* and ADA-deficient mice were remarkably similar, with each manifesting macrophage- and eosinophil-rich inflammation, mucus metaplasia, alveolar enlargement, and tissue fibrosis. As a result of these similarities we hypothesized that similar mechanisms might be important in the generation of the phenotypes in both of these modeling systems. Support for this hypothesis was obtained from the studies noted above that demonstrate that IL-13 is a potent stimulator of adenosine accumulation and that adenosine plays an important role in the pathogenesis of the IL-13 phenotype. Importantly, we also demonstrated that elevated levels of adenosine in ADA-deficient mice stimulated IL-13 elaboration and that this stimulation was mediated by adenosine and an adenosine receptor–mediated pathway. When viewed in combination, these studies highlight a positive feedback loop in which IL-13 increases adenosine accumulation, and adenosine, in turn, induces additional IL-13 elaboration. When this is combined with our observation that IL-13 selectively enhances the expression of adenosine receptors with proinflammatory and bronchospastic properties (A_1, A_{2B}, and A_3), one can easily see how IL-13 and adenosine generate an autoinductive cycle that would amplify and perpetuate inflammation and its fibrotic sequelae and could induce or exaggerate bronchospasm. A positive-feedback loop of this sort could contribute to the nature, chronicity, intensity, and progression of the inflammation, remodeling, and physiologic dysregulation seen in asthma, COPD, and other inflammatory and fibrotic disorders. It is particularly appealing to speculate that this sort of an amplification process could be initiated and could be a dangerous pathogenetic mechanism in diseases such as status asthmaticus and bronchospastic exacerbations of COPD.

IL-13 was originally described as an IL-4–like cytokine and noted to have effector properties relevant to Th2 inflammation. More recent studies demonstrated that IL-13 is a powerful regulator of tissue inflammation and remodeling (28, 29, 53) and implicated IL-13 in the pathogenesis of the inflammatory and remodeling responses in a variety of human disorders including asthma, COPD, IPF, scleroderma, schistosomiasis, and nodular sclerosing Hodgkin disease (30–32, 54). In the present study we demonstrate that chronic IL-13 elaboration is associated with an impressive increase in adenosine in pulmonary tissues and that this adenosine accumulation plays an important role in controlling the intensity and magnitude of IL-13–induced pulmonary inflammation and remodeling. We also demonstrate that IL-13 inhibits ADA enzyme activity and mRNA accumulation while stimulating the expression of adenosine receptors (A_1, A_{2B}, and A_3) that enhance tissue inflammation and bronchospastic responses. Lastly, these studies highlight a potentially important positive-feedback loop, with IL-13 inducing adenosine, while adenosine, in turn, stimulates IL-13 elaboration. As a result of these observations it is reasonable to believe that IL-13–induced adenosine and adenosine-induced IL-13 production play important roles in the pathogenesis of asthma, COPD, and other IL-13–mediated disorders. This establishes ADA enzyme therapy or approaches that intervene in specific adenosine receptor–signaling pathways as novel therapeutic approaches that may be of significant therapeutic use in the treatment of these important diseases.

Acknowledgments

We thank Enzon Inc. for their kind gift of PEG-ADA (Adagen). This work was supported by NIH grants AI-43572 and HL-61888 to M.R. Blackburn and HL-56389, HL-61904, and HL-64242 to J.A. Elias. M.R. Blackburn was also supported by a Junior Investigator Award from the Sandler Family Supporting Foundation.

1. Bradding, P., Redington, A.E., and Holgate, S.T. 1997. Airway wall remodelling in the pathogenesis of asthma: cytokine expression in the airways. In *Airway wall remodelling in asthma*. A.G. Stewart, editor. CRC Press Inc. Boca Raton, Florida, USA. 29–63.
2. Elias, J.A., Zhu, Z., Chupp, G., and Homer, R.J. 1999. Airway remodeling in asthma. *J. Clin. Invest.* **104**:1001–1006.
3. Wallace, W.A., Ramage, E.A., Lamb, D., and Howie, S.E. 1995. A type 2 (Th2-like) pattern of immune response predominates in the pulmonary interstitium of patients with cryptogenic fibrosing alveolitis (CFA). *Clin. Exp. Immunol.* **101**:436–441.
4. Belperio, J.A., et al. 2002. Interaction of IL-13 and C10 in the pathogenesis of bleomycin-induced pulmonary fibrosis. *Am. J. Respir. Cell Mol. Biol.* **27**:419–427.
5. Cosio, M.G., and Guerassimov, A. 1999. Chronic obstructive pulmonary disease. *Am. J. Respir. Crit. Care Med.* **160**(Suppl.):S21–S25.
6. O'Byrne, P.M., and Postma, D.S. 1999. The many faces of airway inflammation: asthma and chronic obstructive pulmonary disease. *Am. J. Respir. Crit. Care Med.* **159**(Suppl.):S41–S66.
7. Saetta, M., et al. 1994. Airway eosinophilia in chronic bronchitis during exacerbations. *Am. J. Respir. Crit. Care Med.* **150**:1646–1652.
8. Senior, R.M., and Shapiro, S.D. 1998. Chronic obstructive pulmonary disease: epidemiology, pathophysiology, and pathogenesis. In *Fishman's pulmonary diseases and disorders*. A.P. Fishman, et al., editors. McGraw-Hill Inc. New York, New York, USA. 659–681.
9. Belardinelli, L., Linden, J., and Berne, R.M. 1989. The cardiac effects of adenosine. *Prog. Cardiovasc. Dis.* **32**:73–97.
10. Fredholm, B.B., and Dunwiddie, T.V. 1988. How does adenosine inhibit transmitter release? *Trends Pharmacol. Sci.* **9**:130–134.
11. Churchill, P.C. 1982. Renal effects of 2-chloroadenosine and their antagonism by aminophylline in anesthetized rats. *J. Pharmacol. Exp. Ther.* **222**:319–323.
12. Huang, S., Apasov, S., Koshiba, M., and Sitkovsky, M. 1997. Role of A2a extracellular adenosine receptor-mediated signaling in adenosine-mediated inhibition of T-cell activation and expansion. *Blood.* **90**:1600–1610.
13. Okusa, M.D., Linden, J., Macdonald, T., and Huang, L. 1999. Selective A2A adenosine receptor activation reduces ischemia-reperfusion injury in rat kidney. *Am. J. Physiol.* **277**:F404–F412.
14. Ohta, A., and Sitkovsky, M. 2001. Role of G-protein-coupled adenosine receptors in downregulation of inflammation and protection from tissue damage. *Nature.* **414**:916–920.
15. Tilley, S.L., Wagoner, V.A., Salvatore, C.A., Jacobson, M.A., and Koller, B.H. 2000. Adenosine and inosine increase cutaneous vasopermeability by activating A(3) receptors on mast cells. *J. Clin. Invest.* **105**:361–367.
16. Driver, A.G., Kukoly, C.A., Ali, S., and Mustafa, S.J. 1993. Adenosine in bronchoalveolar lavage fluid in asthma. *Am. Rev. Respir. Dis.* **148**:91–97.
17. Marquardt, D.L., Parker, C.W., and Sullivan, T.J. 1978. Potentiation of mast cell mediator release by adenosine. *J. Immunol.* **120**:871–878.
18. Walker, B.A., et al. 1997. Adenosine A3 receptor expression and function in eosinophils. *Am. J. Respir. Cell Mol. Biol.* **16**:531–537.

19. Hasko, G., et al. 1996. Adenosine receptor agonists differentially regulate IL-10, TNF-alpha, and nitric oxide production in RAW 264.7 macrophages and in endotoxemic mice. *J. Immunol.* **157**:4634–4640.
20. Bai, T.R., Lam, R., and Prasad, F.Y. 1989. Effects of adrenergic agonists and adenosine on cholinergic neurotransmission in human tracheal smooth muscle. *Pulm. Pharmacol.* **1**:193–199.
21. Johnson, H.G., and McNee, M.L. 1985. Adenosine-induced secretion in the canine trachea: modification by methylxanthines and adenosine derivatives. *Br. J. Pharmacol.* **86**:63–67.
22. Ali, S., Mustafa, S.J., and Metzger, W.J. 1994. Adenosine-induced bronchoconstriction and contraction of airway smooth muscle from allergic rabbits with late-phase airway obstruction: evidence for an inducible adenosine A1 receptor. *J. Pharmacol. Exp. Ther.* **268**:1328–1334.
23. Cushley, M.J., Tattersfield, A.E., and Holgate, S.T. 1983. Inhaled adenosine and guanosine on airway resistance in normal and asthmatic subjects. *Br. J. Clin. Pharmacol.* **15**:161–165.
24. Oosterhoff, Y., de Jong, J.W., Jansen, M.A., Koeter, G.H., and Postma, D.S. 1993. Airway responsiveness to adenosine 5′-monophosphate in chronic obstructive pulmonary disease is determined by smoking. *Am. Rev. Respir. Dis.* **147**:553–558.
25. Blackburn, M.R., et al. 2000. Metabolic consequences of adenosine deaminase deficiency in mice are associated with defects in alveogenesis, pulmonary inflammation, and airway obstruction. *J. Exp. Med.* **192**:159–170.
26. Chunn, J.L., Young, H.W., Banerjee, S.K., Colasurdo, G.N., and Blackburn, M.R. 2001. Adenosine-dependent airway inflammation and hyperresponsiveness in partially adenosine deaminase-deficient mice. *J. Immunol.* **167**:4676–4685.
27. Vestbo, J., and Prescott, E. 1997. Update on the "Dutch hypothesis" for chronic respiratory disease. *Lancet.* **350**:1431–1434.
28. Zheng, T., et al. 2000. Inducible targeting of IL-13 to the adult lung causes matrix metalloproteinase- and cathepsin-dependent emphysema. *J. Clin. Invest.* **106**:1081–1093.
29. Zhu, Z., et al. 1999. Pulmonary expression of interleukin-13 causes inflammation, mucus hypersecretion, subepithelial fibrosis, physiologic abnormalities and eotaxin production. *J. Clin. Invest.* **103**:779–788.
30. Chiramonte, M.G., Donaldson, D.D., Cheever, A.W., and Wynn, T.A. 1999. An IL-13 inhibitor blocks the development of hepatic fibrosis during a T-helper type 2-dominated inflammatory response. *J. Clin. Invest.* **104**:777–785.
31. Hancock, A., Armstrong, L., Gama, R., and Millar, A. 1998. Production of interleukin 13 by alveolar macrophages from normal and fibrotic lung. *Am. J. Respir. Cell Mol. Biol.* **18**:60–65.
32. Hasegawa, M., Fujimoto, M., Kikuchi, K., and Takehara, K. 1997. Elevated serum levels of interleukin 4 (IL-4), IL-10, and IL-13 in patients with systemic sclerosis. *J. Rheumatol.* **24**:328–332.
33. Zhu, Z., et al. 2002. IL-13-induced chemokine responses in the lung: role of CCR2 in the pathogenesis of IL-13-induced inflammation and remodeling. *J. Immunol.* **168**:2953–2962.
34. Blackburn, M.R., Datta, S.K., and Kellems, R.E. 1998. Adenosine deaminase-deficient mice generated using a two-stage genetic engineering strategy exhibit a combined immunodeficiency. *J. Biol. Chem.* **273**:5093–5100.
35. Knudsen, T.B., et al. 1992. Effects of (R)-deoxycoformycin (pentostatin) on intrauterine nucleoside catabolism and embryo viability in the pregnant mouse. *Teratology.* **45**:91–103.
36. Blackburn, M.R., et al. 2000. The use of enzyme therapy to regulate the metabolic and phenotypic consequences of adenosine deaminase deficiency in mice. Differential impact on pulmonary and immunologic abnormalities. *J. Biol. Chem.* **275**:32114–32121.
37. Winston, J.H., Hanten, G.R., Overbeek, P.A., and Kellems, R.E. 1992. 5′ flanking sequences of the murine adenosine deaminase gene direct expression of a reporter gene to specific prenatal and postnatal tissues in transgenic mice. *J. Biol. Chem.* **267**:13472–13479.
38. Lee, C.G., et al. 2001. Interleukin-13 induces tissue fibrosis by selectively stimulating and activating TGF-β_1. *J. Exp. Med.* **194**:809–821.
39. Lee, C.G., et al. 2002. Transgenic overexpression of IL-10 in the lung causes mucus metaplasia, tissue inflammation and airways remodeling via IL-13-dependent and -independent pathways. *J. Biol. Chem.* **277**:35466–35474.
40. Banerjee, S.K., Young, H.W., Volmer, J.B., and Blackburn, M.R. 2002. Gene expression profiling in inflammatory airway disease associated with elevated adenosine. *Am. J. Physiol. Lung Cell Mol. Physiol.* **282**:L169–L182.
41. Albrecht, U., Eichele, G., Helms, J., and Lu, H. 1997. Visualization of gene expression patterns by in situ hybridization. In *Molecular and cellular methods in developmental toxicology*. G. Daston, editor. CRC Press Inc. Boca Raton, Florida, USA. 23–48.
42. Wakamiya, M., et al. 1995. Disruption of the adenosine deaminase gene causes hepatocellular impairment and perinatal lethality in mice. *Proc. Natl. Acad. Sci. U. S. A.* **92**:3673–3677.
43. Blackburn, M.R., and Kellems, R.E. 1996. Regulation and function of adenosine deaminase in mice. *Prog. Nucleic Acid Res. Mol. Biol.* **55**:195–226.
44. Fredholm, B.B., et al. 2001. International Union of Pharmacology. XXV. Nomenclature and classification of adenosine receptors. *Pharmacol. Rev.* **53**:527–552.
45. Perez-Rodriguez, E., and Jimenez Castro, D. 2000. The use of adenosine deaminase and adenosine deaminase isoenzymes in the diagnosis of tuberculous pleuritis. *Curr. Opin. Pulm. Med.* **6**:259–266.
46. Andersen, P. 1994. The T cell response to secreted antigens of Mycobacterium tuberculosis. *Immunobiology.* **191**:537–547.
47. Linden, J. 2001. Molecular approach to adenosine receptors: receptor-mediated mechanisms of tissue protection. *Annu. Rev. Pharmacol. Toxicol.* **41**:775–787.
48. Feoktistov, I., and Biaggioni, I. 1995. Adenosine A2b receptors evoke interleukin-8 secretion in human mast cells. An enprofylline-sensitive mechanism with implications for asthma. *J. Clin. Invest.* **96**:1979–1986.
49. Salvatore, C.A., et al. 2000. Disruption of the A(3) adenosine receptor gene in mice and its effect on stimulated inflammatory cells. *J. Biol. Chem.* **275**:4429–4434.
50. Kondo, A., Isaji, S., Nishimura, Y., and Tanaka, T. 2000. Transcriptional and post-transcriptional regulation of monocyte chemoattractant protein-3 gene expression in human endothelial cells by phorbol ester and cAMP signalling. *Immunology.* **99**:561–568.
51. Kotsimbos, T.C., Ernst, P., and Hamid, Q.A. 1996. Interleukin-13 and interleukin-4 are coexpressed in atopic asthma. *Proc. Assoc. Am. Physicians.* **108**:368–373.
52. Zhu, Z., Ma, B., Homer, R.J., Zheng, T., and Elias, J.A. 2001. Use of the tetracycline-controlled transcriptional silencer (tTS) to eliminate transgene leak in inducible overexpression transgenic mice. *J. Biol. Chem.* **276**:25222–25299.
53. Wills-Karp, M., et al. 1998. Interleukin-13: central mediator of allergic asthma. *Science.* **282**:2258–2260.
54. Ohshima, K., et al. 2001. Interleukin-13 and interleukin-13 receptor in Hodgkin's disease: possible autocrine mechanism and involvement in fibrosis. *Histopathology.* **38**:368–375.